UNCERTAINTY QUANTIFICATION IN REACTING FLOWS

S. Ruoff*, B. Enderle*, G. Eckel*, B. Rauch*, T. Methling*, P. Le Clercq*

* German Aerospace Center (DLR), Institute of Combustion Technology, Pfaffenwaldring 38-40, 70569 Stuttgart, Germany

Abstract

One source of input uncertainties in the simulation of turbulent spray combustion is introduced by the choice of surrogate species, which link the liquid and the gaseous phase. To support the certification of novel jet fuels and enhance the predictive capabilities of such simulations, output uncertainties should be disclosed. Therefore, the paper at hand quantifies the impact of the choice of surrogate species on typical flame characteristics (laminar flame speed, ignition delay times) in simplified 0-D and 1-D flames. On the basis of the results two cases are selected to determine the impact of the uncertainties in the laminar flame speeds on a flame in an atmospheric, generic, swirl-stabilized spray burner. The uncertainties are propagated by adjusting the Arrhenius coefficients of the utilized chemical reaction mechanism. As a result, the heat release zone in the combustion chamber is closer to the burner inlet for greater laminar flame speeds, and thus the flame is more compact.

Keywords

Uncertainity Quantification, CFD, Multiphase Combustion, Surrogate Species

1. INTRODUCTION

Jet engines and gas turbines are highly complex machines whose functionality is described and ruled by the interaction of nearly all engineering disciplines. The complexity is reflected by strict certification processes that review every aspect of the operation of such systems. Especially in regards to the introduction of novel fuels the certification plays a major role [1]. The immense costs for the development of gas turbines and engines as well as the expensive and lengthy certification of novel jet fuels can be reduced by a focused and well-planned application of highly accurate numerical simulations. While doing so it is important to identify and quantify possible uncertainties in the simulation.

One major aspect for the certification of novel jet fuels is the combustion of the liquid fuels in the jet engine [2]. The combustion of turbulent sprays consist of many complex, interacting sub-processes such as primary and secondary atomization, evaporation or turbulence-chemistry interaction. Thus, there are many potential sources of uncertainty, one of which is the selection of the so-called surrogate species representing the fuel.

Since a typical Jet A-1 fuel consists of hundreds of different components, it would be computationally expensive to model every single one of them. In many cases, the fuel is modelled by a surrogate approach, using a small number of selected species (e.g. [3, 4]) that represent typical chemical (e.g. laminar flame speeds, ignition delay times, H/C ratio) and physical properties (e.g. density, distillation curve) of the jet fuel [5]. This approach already leads to uncertainties, e.g. for the sooting behavior depending on the choice of the species representing aromatics [6].

However, other uncertainties are introduced if some liquid fuel components are not present in the available chemical reaction mechanism(s) or if the chemical reaction mechanism consists of multiple species of the same fuel family. To quantify the influence of these uncertainties, a sensitivity analysis for the fuel mapping (choice of equivalent species) on the laminar flame speed S_L and the ignition delay time (t_{ign}) is investigated. Based on the results of the sensitivity analysis, the introduced errors in the laminar flame speeds are propagated to a multiphase combustion case, where the isolated influence of the laminar flame speed on typical flame characteristics is quantified.

2. NUMERICAL MODELLING

In the following section the numerical models will be introduced briefly. The main focus will be on the mapping of fuels between the liquid and gaseous phase. Simulations ar carried out using Cantera [7] for the generic test cases and the DLR in-house simulation framework ThetaCOM-SPRAYSIM [8, 9] for the complex, multiphase computational fluid dynamics (CFD) simulations.

2.1. Gas phase modelling

The gaseous phase is simulated by the DLR in-house code ThetaCOM, which employs a 3D finite-volume

solver for unstructured grids. The underlying equations are the conservation of mass, momentum, species and enthalpy. The species conservation equation

$$\frac{\partial}{\partial t}\int_v \rho_g Y_\alpha dv + \int_s \rho_g Y_\alpha \mathbf{u}\cdot\mathbf{n}ds + \int_s \mathbf{J}_\alpha\cdot\mathbf{n}ds = \int_v S_{Y_\alpha}dv + \int_v S^d_{Y_\alpha}dv \tag{1}$$

with the species source term $S^d_{Y_\alpha}$ due to the presence of liquid droplets and the species source S_{Y_α} due to chemical reactions illustrates the coupling between the gaseous phase and the liquid and chemical source terms, respectively. Every gaseous species present in the chemical mechanism is accounted for in Eq. 1.

2.2. Chemical reactions mechanism

The chemical reaction kinetics are described by Arrhenius laws (Eq. 2) for the rate constants

$$k(T) = AT^b exp\left(\frac{-E_A}{RT}\right) \tag{2}$$

where A is the pre-exponential factor, b is the temperature exponent, E_A is the activation energy and R the universal gas constant.

The chemical reaction mechanism utilized in the paper at hand was developed by the CRECK group of the Politecnico di Milano [10], adapted for jet fuels of the JETSCREEN program [11], as described in [5, 12]. The different main fuel species available in the mechanism are listed in the third column ("Equivalent species") of Tab. 1

For CFD simulations, the computational costs increase with an increasing size of the reaction mechanism, i.e. number of species and number of reactions. To lower the computational costs, the mechanisms are reduced by cutting out some species and reactions. However, this can lead to inaccuracies in the resulting flame characteristics. To compensate these inaccuracies, the DLR in-house tool linTM [13] is used. After the reduction of the mechanism, linTM adjusts the Arrhenius constants (Eq. 2) of chosen reaction equations to re-obtain the accuracy of the original mechanism.

2.3. Liquid phase modelling

The liquid phase is modelled by the continuous thermodynamics model (CTM) [14, 15]. It assumes that the species distribution of complex fuels that are composed of hundreds of different species can be approximated by a continuous description via probability density functions. The fuel components are grouped into fuel families, as shown exemplarily in Fig. 1. In the paper at hand, the probability density function (PDF) of each family follows a Γ-distribution. This reduces the number of degrees of freedom in

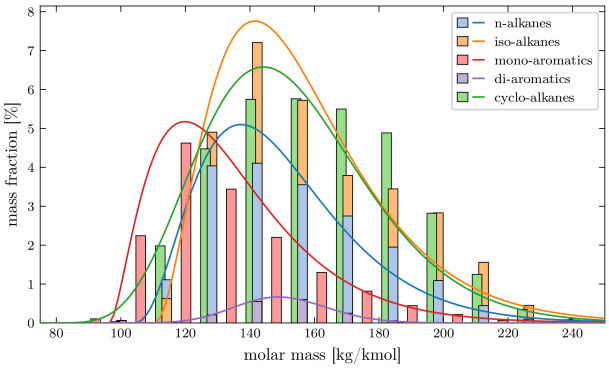

FIG 1. Fuel composition for a conventional jet fuel clustered by fuel families. Bars indicate the discrete composition, lines the fitted composition by gamma distribution.

the evaporation model by orders of magnitude, which cuts down the computational costs.

The coupling between the liquid and gaseous phase is accomplished via source terms. Regarding the liquid source term $S^d_{Y_\alpha}$ in Eq. 1, there is no one-to-one mapping as for the chemical reaction source terms. For each liquid fuel family, one so called equivalent species in the chemical mechanism has to be selected. Only the equivalent gaseous species obtains the droplet sources of the whole fuel family it is assigned to. For the investigated fuel, there are four fuel families in the liquid phase (n-alkanes, iso-alkanes, $cyclo$-alkanes and aromatics), that can be mapped to four equivalent species. If, for example $i\mathrm{C_{12}H_{26}}$ is selected as equivalent species for the family of iso-alkanes, all the mass evaporated in the liquid phase solver contributes to the source term of $i\mathrm{C_{12}H_{26}}$ only, independent of other iso-alkanes present in the chemical reaction mechanism. Tab. 1 list all of the available equivalent species in the mechanism at hand, that correspond to the fuel family in the liquid phase.

CTM fuel family	mole fraction	Equivalent species
n-alkanes	0.19	$n\mathrm{C_{10}H_{22}}$
		$n\mathrm{C_{10}H_{22}}$
		$n\mathrm{C_{10}H_{22}}$
iso-alkanes	0.31	$i\mathrm{C_8H_{18}}$
		$i\mathrm{C_{12}H_{26}}$
		$i\mathrm{C_{16}H_{34}}$
$cyclo$-alkanes	0.33	Decalin
		Methylcyclohexan
aromatics	0.17	Trimethylbenzene
		Xylene
		Toluene
		N-Butylbenzene

TAB 1. Fuel composition and available selection of equivalent species

3. TEST CASES

In the following section the three numerical test cases for the calculation of the laminar flame speed, ignition delay time and multiphase-flow are briefly introduced.

3.1. Laminar Flame Speed

The laminar flame speed (S_L) is defined as the propagation velocity of a flame front into an unburned gas mixture. In contrast to the experimental configuration using a premixed conical shaped flame [16], in the numerical case it is determined using a 1-D flame outlined in Fig. 2. The 1-D case [7] consists of a freely-

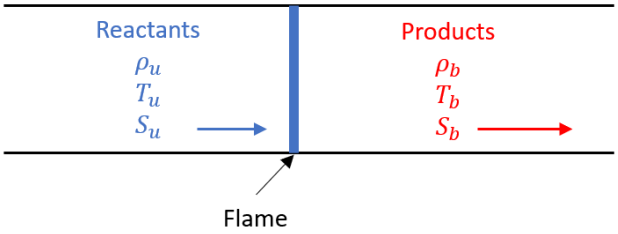

FIG 2. Setup of 1-D flame in a flame fixed coordinate system.

propagating, adiabatic flame, where the reactants enter the domain with (unburnt) density ρ_u, temperature T_u and speed S_u. In the flame-fixed coordinate system the product exit the domain with (burnt) density ρ_b, temperature T_b and speed S_b. In this case, the laminar flame speed S_L is equivalent to the (unburnt) inlet velocity S_u. To determine the flame speed, the steady state problem is solved by Newton's method, where computational domain is iteratively expanded and the grid points refined.
The laminar flame speed depends on the temperature, pressure and equivalence ratio ϕ. The calculations for the flame speed were carried out at constant pressure of $1\,\mathrm{bar}$ and temperature of $473\,\mathrm{K}$. The equivalence ratio ranges from 0.6 to 1.3.

3.2. Ignition Delay Time

In addition to the laminar flame speed, the ignition delay time is a fundamental combustion property. It is defined as the time period between the onset of the reactive system by a shock wave and the onset of ignition [17]. Measurements are usually performed in a shock tube, the delay time is defined as the time between the initiation of the reactive system and the peak of CH*-radical concentration [17].
The numerical prediction of the ignition delay time is achieved by modelling the shock tube with a constant volume, adiabatic reactor. In contrast to the experiments, the ignition delay time is determined by the peak in OH concentration.

3.3. Multiphase Test Case: DLR Standard Spray Burner

Fig. 3 shows the numerical representation of the DLR Standard Spray Burner (SSB). The experimental setup can be found in [18]. The combustor consist of a pre-filming airblast atomizer, whose inner and outer swirler creates two co-axial, co-rotating swirling air flows. The cross section of the combustion chamber is $85\,\mathrm{mm} \times 85\,\mathrm{mm}$, its height $196\,\mathrm{mm}$ and the exit on top is circular with a diameter of $40\,\mathrm{mm}$. The compu-

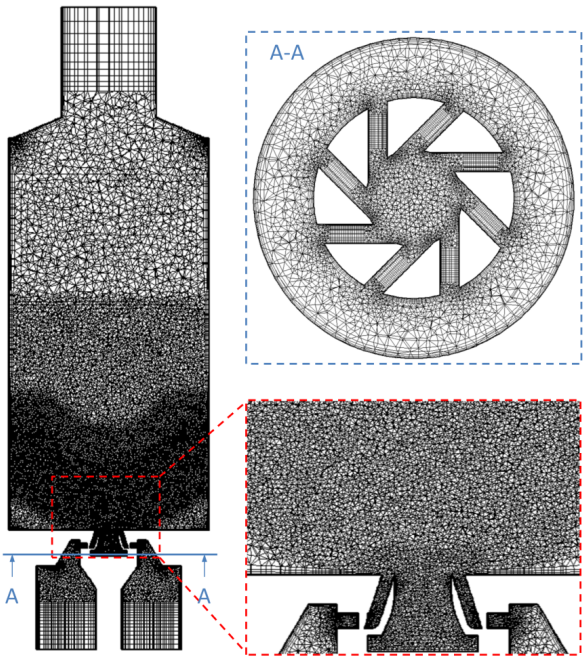

FIG 3. Computational grid of the DLR Standard Spray Burner

tational domain is discretized by a fully unstructured tetrahedral mesh, which is refined within the swirler vanes, the mixing zone and in the region where the flame resides.

4. SENSITIVITY ANALYSIS

To determine which fuel families and properties have the largest influence on the laminar flame speed S_L and the ignition delay time t_{ign}, a parametric study is conducted. The input parameters are the different equivalent species listed in Tab. 1, which results in a total number of 72 samples. Usually, the input parameters for a sampling are continuous variables, where a larger number of samples can be drawn, which is not possible for the discrete nature of the choice of equivalent species. This leads to a relatively small sample size and thus no reliable sensitivity coefficients. Therefore, the sensitivities are estimated via scatter plots and linear regression fits.
The results of the sensitivity analysis are shown in Fig. 4 as scatter plot. For each species of a fuel family, the corresponding samples and results for S_L and t_{ign} are shown as dots. For the laminar flame speeds there is no evident trend for any of the fuel families. However, the choice of the $cyclo$-alkanes has the lowest spread within each of its equivalent species, indicating that it has the largest influence.

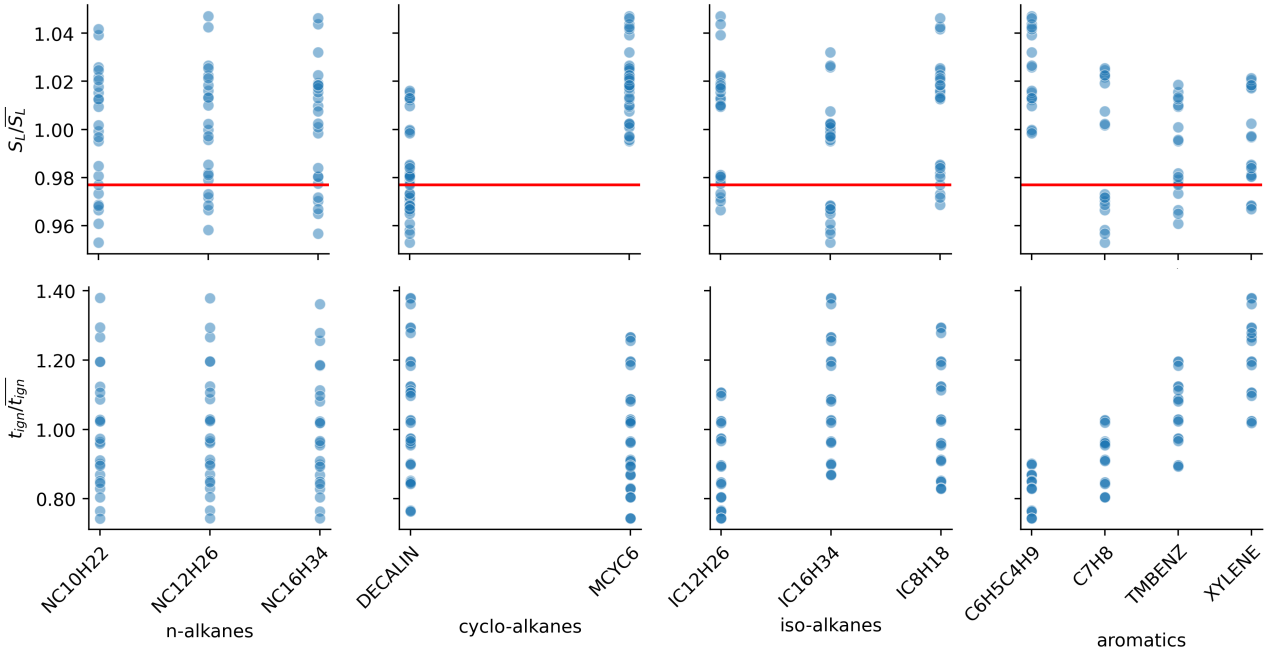

FIG 4. Dependency of normalized laminar flame speed S_L (top row) and normalized ignition delay time t_{ign} (bottom row) on chosen equivalent species. Each dot symbolizes one set of parameters, the line is the measured laminar flame speed.

For the ignition delay time, there seems to be a clear trend towards the choice of the aromatics' equivalent fuel species. Similar to the $cyclo$-alkanes for S_L, the spread for each species in the aromatics is lowest among the fuel families. However, the apparent linear trend for the aromatics can be misleading, since the fuel species are sorted alphanumerically. Therefore, the ignition delay time is most sensitive to the choice of the aromatic equivalent species, but there is no indicator on which property of the fuel species leads to the change in t_{ign}. To further elaborate which properties of the equivalent species lead to the changes in S_L and t_{ign}, a linear regression is made for some properties. Fig. 5 shows the samples, but this time as function of the properties of the fuel mixture. For the laminar flame speed, a clear sensitivity can be observed towards the C/H-ratio of the fuel, the heat capacity (c_p) and the higher heating value (HHV). Thus, if one of the aforementioned properties of the equivalent species changes, it also alters the laminar flame speed. The ignition delay time however does not seem to be sensitive to the chosen properties, indicated by the large spread of the samples and the larger confidence intervals of the regression fits.

5. ERROR PROPAGATION TO MULTIPHASE CFD

As discussed in the previous section, the choice of the equivalent species influences the laminar flame speed S_L. To quantify the uncertainties that the variance of S_L has on a lab-scale spray flame, a second study is conducted for the DLR SSB.

5.1. Error propagation

Initially, the choice of the equivalent species is the source of uncertainties and the laminar flame speed merely a dependent variable that is not directly an input to the CFD simulation. But since the laminar flame speed is an important measure in the assessment of kinetic reaction mechanisms, the influence of its variance on a complex flame is of interest.

Since a full parametric study as in the previous section would be too computationally expensive for a multiphase CFD simulation, the uncertainty in S_L is used as direct input for the uncertainty quantification. This has two advantages:

- An already reduced reaction mechanisms (50 species, 426 reactions) can be used instead of the original mechanism (463 species, 13829 reactions), which reduces the computational costs.
- The influence of S_L can be investigated independent from any other parameters, since changes in the equivalent species lead to changes in other parameters (e.g. t_{ign}, C/H-ratio).

However, the variation of the laminar flame speed is not trivial, since it is no direct input parameter. To propagate the uncertainties in S_L to the CFD, the chemical reaction mechanism is adjusted. By changing the pre-exponential factor A in Eq. 2 of reactions with the highest sensitivity towards S_L, the laminar flame speed can be altered. The manipulation of the reactions is again achieved with the DLR tool linTM and the changes are listed in Tab. 2. That way, the reduced mechanism is adjusted to fit the minimum and maximum laminar flame speed from the sensitivity analysis (Fig. 6, red and blue dashed lines). The new, modified reduced mechanisms are

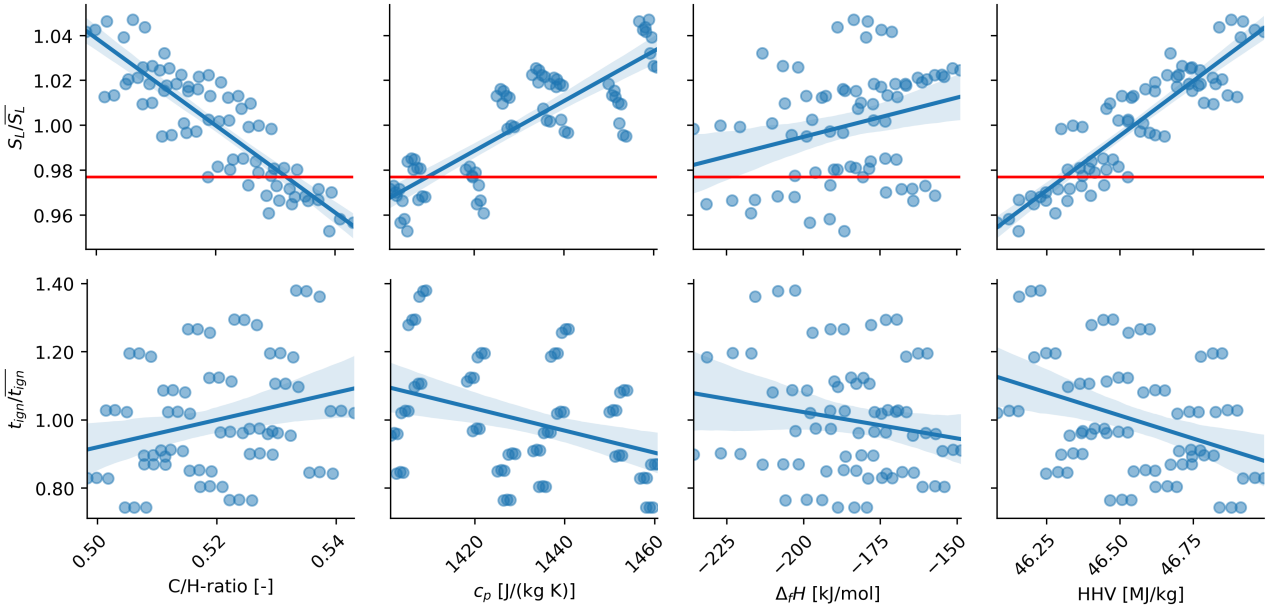

FIG 5. Dependency of normalized laminar flame speed S_L (top row) and normalized ignition delay time t_{ign} (bottom row) on different properties of the fuel. Each dot symbolizes one set of parameters, blue lines represent the linear regression fit, red line is the measured laminar flame speed.

Reaction	A_{ref}	A_{max}	A_{min}
$H + O_2 \Leftrightarrow O + OH$	$9.452 \cdot 10^{15}$	$1.138 \cdot 10^{16}$	$7.886 \cdot 10^{15}$
$OH + CO \Leftrightarrow H + CO_2$	$1.265 \cdot 10^{10}$	$1.465 \cdot 10^{10}$	$1.058 \cdot 10^{10}$

TAB 2. Changes in reaction mechanism to account for variance in the laminar flame speed

then used to perform two simulations, one for the minimum and one for the maximum laminar flame speed.

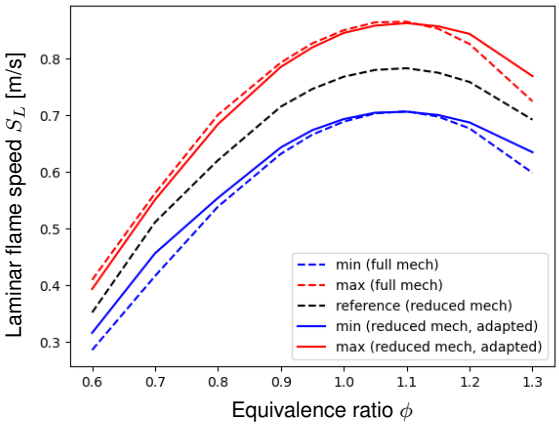

FIG 6. Upper and lower bounds of S_L due to the choice of equivalent species.

5.2. Results

Since only two simulations for the minimum and maximum laminar flame speeds are performed, there are no statistics available. Nonetheless, the results provide some insights. The heat release zones (Fig. 7) vary in height as well as in their respective position along the z-axis inside the combustion chamber. Due to the lower flame speed, the corresponding reaction zone (Fig. 7b) extends longer into the combustion chamber. Also, the peak in heat release is located slightly further downstream as for the larger flame speed. Furthermore, the maximum heat release is marginally bigger for the maximum flame speed (Fig. 7a) case. At the same time, the z-position of the flame root (lower part of 30% iso-line) is very similar. Moreover, the flame's extent in x-direction does not change either. Compared to previous studies on the influence of the uncertainties of spray starting conditions [19], the uncertainties due to the change in laminar flame speed caused by the choice of different equivalent species is small.

6. CONCLUSION

Numerical simulations can help reduce the costs of certification of novel aviation fuels. Therefore, the uncertainties in the numerical simulations have to be identified and quantified. One source of input uncertainty stems from the choice of the surrogate species representing the jet fuel.

In the paper at hand, the uncertainty on the laminar flame speed and ignition delay time introduced by the choice of the equivalent species was investigated. The mapping of four fuel families in the liquid phase onto 12 different equivalent species in the gaseous phase was done by means of a full parametric study. The results show a clear impact on both output parameters. The flame speed has a large sen-

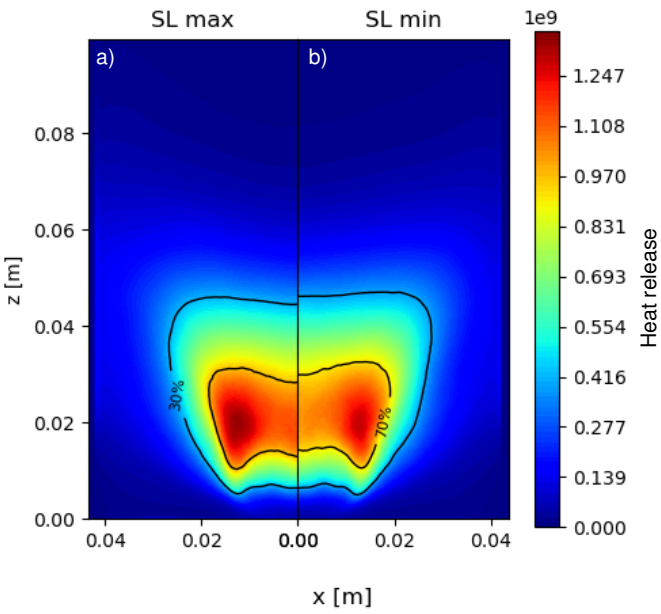

FIG 7. Line of sight integrated heat release, mirrored at $x = 0\,\mathrm{mm}$. The iso lines represent 30% and 70% of the common maximum heat release.

sitivity on the choice of the equivalent species for the $cyclo$-alkane, whereas the ignition delay time has the biggest sensitivity towards the aromatic species. Furthermore, the laminar flame speed seems to correlate with the changes in C/H-ratio, heat capacity and heat of combustion. However, in contrast to the flame speed, the ignition delay time does not seem to corelate with any properties.

To illustrate the impact of changes in the flame speed on a lab-scale flame, the uncertainties are propagated by altering the coefficients of the chemical reaction mechanism. That way, the isolated influence of the flame speed was considered. As a result, the position of heat release and thus the flame length increases with lower laminar flame speeds. At the same time, the output uncertainties due to the change in laminar flame speed is small compared to the uncertainties introduced by uncertainties in spray start conditions from a previous study [19].

The publication aims to provide an approach to quantify the uncertainties introduced by the choice of equivalent species. However, the implications of fuel families not present in a chemical mechanism, leading to lumping of different fuel families into one equivalent species were not considered. Furthermore, a more though analysis, on which fuel properties are responsible for the changes in the output parameters could lead to more insight, on how to best choose the equivalent species. At last, a similar study on the lab-scale flame for uncertainties ignition delay time or other output parameters (e.g. adiabatic flame temperature) is planned.

7. ACKNOWLEDGMENT

The authors kindly acknowledge the support of the German Aerospace Center (DLR) within the project "Simulation Based Certification" (SimBaCon).

Contact address:

stephan.ruoff@dlr.de

References

[1] ASTM D4054-09. Standard practice for qualification and approval of new aviation turbine fuels and fuel additives. Standard, West Conshohocken, PA, 2009.

[2] M. Colket, J. Heyne, M. Rumizen, M. Gupta, T. Edwards, W. M. Roquemore, G. Andac, R. Boehm, J. Lovett, R. Williams, J. Condevaux, D. Turner, N. Rizk, J. Tishkoff, C. Li, J. Moder, D. Friend, and V. Sankaran. Overview of the National Jet Fuels Combustion Program. *AIAA Journal*, 55(4):1087–1104, 2017. DOI: 10.2514/1.J055361.

[3] V. Shastry, Q. Cazères, B. Rochette, E. Riber, and B. Cuenot. Numerical study of multicomponent spray flame propagation. *Proceedings of the Combustion Institute*, 38(2):3201–3211, 2020 // 2021. DOI: 10.1016/j.proci.2020.07.090.

[4] H. Wang, R. Xu, K. Wang, C. T. Bowman, R. K. Hanson, D. F. Davidson, K. Brezinsky, and F. N. Egolfopoulos. A physics-based approach to modeling real-fuel combustion chemistry - I. Evidence from experiments, and thermodynamic, chemical kinetic and statistical considerations. *Combustion and Flame*, 193:502–519, 2018. DOI: 10.1016/j.combustflame.2018.03.019.

[5] M. Pelucchi, P. Oßwald, W. Pejpichestakul, A. Frassoldati, and M. Mehl. On the combustion and sooting behavior of standard and hydrotreated jet fuels: An experimental and modeling study on the compositional effects. *Proceedings of the Combustion Institute*, 38(1):523–532, 2021. DOI: 10.1016/j.proci.2020.06.353.

[6] A. Mensch, R. J. Santoro, T. A. Litzinger, and S.-Y. Lee. Sooting characteristics of surrogates for jet fuels. *Combustion and Flame*, 157(6):1097–1105, 2010. DOI: 10.1016/j.combustflame.2010.02.008.

[7] D. G. Goodwin, H. K. Moffat, I. Schoegl, R. L. Speth, and B. W. Weber. Cantera: An object-oriented software toolkit for chemical kinetics, thermodynamics, and transport processes. `https://www.cantera.org`, 2022. Version 2.6.0. DOI: 10.5281/zenodo.6387882.

[8] M. Di Domenico, P. Gerlinger, and B. Noll. Numerical simulations of confined, turbulent, lean,

premixed flames using a detailed chemistry combustion model. In *ASME 2011 Turbo Expo: Turbine Technical Conference and Exposition*, pages 519–530. ASME Digital Collection, 2011.

[9] G. Eckel, M. Rachner, P. Le Clercq, and M. Aigner. Semi-empirical model for the unsteady shear breakup of liquid jets in cross-flow. *Atomization and Sprays*, 26(7), 2016.

[10] E. RANZI, A. Frassoldati, A. STAGNI, M. Pelucchi, A. Cuoci, and T. FARAVELLI. Reduced Kinetic Schemes of Complex Reaction Systems: Fossil and Biomass-Derived Transportation Fuels. *International Journal of Chemical Kinetics*, 46(9):512–542, 2014. DOI: 10.1002/kin.20867.

[11] JETSCREEN. JET Fuel SCREENing and Optimization, 2020. 06.2017–10.2020, European Union's Horizon 2020 research and innovation programme under grant agreement No 723525.

[12] M. Mehl and M. Pelucchi. D2.5 - Report about the high temperature regime regarding autoignition, combustion and soot. JETSCREEN project deliverable.

[13] T. Methling, M. Braun-Unkhoff, and U. Riedel. A novel linear transformation model for the analysis and optimisation of chemical kinetics. *Combustion Theory and Modelling*, 21(3):503–528, 2017. DOI: 10.1080/13647830.2016.1251616.

[14] P. Le Clercq, N. Doué, M. Rachner, and M. Aigner. Validation of a multicomponent-fuel model for spray computations. In *47th AIAA Aerospace Sciences Meeting including The New Horizons Forum and Aerospace Exposition*, page 1188, 2009.

[15] N. Doué, P. Le Clercq, and M. Aigner. Validation of a multicomponent-fuel droplet evaporation model based on continuous thermodynamics. In *International Congress on Liquid Atomization and Spray Systems*, 2006.

[16] S. Richter, M. B. Raida, C. Naumann, and U. Riedel, editors. *Measurement of the laminar burning velocity of neat jet fuel components*, 2016.

[17] P. Dagaut, F. Karsenty, G. Dayma, P. Diévart, K. Hadj-Ali, A. Mzé-Ahmed, M. Braun-Unkhoff, J. Herzler, T. Kathrotia, T. Kick, C. Naumann, U. Riedel, and L. Thomas. Experimental and detailed kinetic model for the oxidation of a Gas to Liquid (GtL) jet fuel. *Combustion and Flame*, 161(3):835–847, 2014. DOI: 10.1016/j.combustflame.2013.08.015.

[18] J. Grohmann, W. O'Loughlin, W. Meier, and M. Aigner. Comparison of the Combustion Characteristics of Liquid Single-Component Fuels in a Gas Turbine Model Combustor. In *Turbo Expo: Power for Land, Sea, and Air*, New York, N.Y., 2016. American Society of Mechanical Engineers. DOI: 10.1115/GT2016-56177.

[19] B. Enderle. Uncertainty quantification in the simulation of turbulent spray combustion. DOI: 10.18419/opus-12004.